The Journal of Immunology

RESEARCH ARTICLE | SEPTEMBER 01 2005

Wild-Type Measles Virus Infection in Human CD46/CD150-Transgenic Mice: CD11c-Positive Dendritic Cells Establish Systemic Viral Infection[1] FREE

Masashi Shingai; ... et. al

J Immunol (2005) 175 (5): 3252–3261.
https://doi.org/10.4049/jimmunol.175.5.3252

Wild-Type Measles Virus Infection in Human CD46/CD150-Transgenic Mice: CD11c-Positive Dendritic Cells Establish Systemic Viral Infection[1]

Masashi Shingai,[2]*† Naokazu Inoue,[2]‡ Tsuyoshi Okuno,‡ Masaru Okabe,‡ Takashi Akazawa,* Yasuhide Miyamoto,* Minoru Ayata,§ Kenya Honda,¶ Mitsue Kurita-Taniguchi,* Misako Matsumoto,*† Hisashi Ogura,§ Tadatsugu Taniguchi,¶ and Tsukasa Seya[3]†

We generated transgenic (TG) mice that constitutively express human CD46 (huCD46) and/or TLR-inducible CD150 (huCD150), which serve as receptors for measles virus (MV). These mice were used to study the spreading and pathogenicity of GFP-expressing or intact laboratory-adapted Edmonston and wild-type Ichinose (IC) strains of MV. Irrespective of the route of administration, neither type of MV was pathogenic to these TG mice. However, in ex vivo, limited replication of IC was observed in the spleen lymphocytes from huCD46/huCD150 TG and huCD150 TG, but not in huCD46 TG and non-TG mice. In huCD150-positive TG mouse cells, CD11c-positive bone marrow-derived myeloid dendritic cells (mDC) participated in MV-mediated type I IFN induction. The level and induction profile of IFN-β was higher in mDC than the profile of IFN-α. Wild-type IC induced markedly high levels of IFN-β compared with Edmonston in mDC, as opposed to human dendritic cells. We then generated huCD46/huCD150 TG mice with type I IFN receptor (IFNAR1)$^{-/-}$ mice. MV-bearing mDCs spreading to draining lymph nodes were clearly observed in these triple mutant mice in vivo by i.p. MV injection. Infectious lymph nodes were also detected in the double TG mice into which MV-infected CD11c-positive mDCs were i.v. transferred. This finding suggests that in the double TG mouse model mDCs once infected facilitate systemic MV spreading and infection, which depend on mDC MV permissiveness determined by the level of type I IFN generated via IFNAR1. Although these results may not simply reflect human MV infection, the huCD150/huCD46 TG mice may serve as a useful model for the analysis of MV-dependent modulation of mDC response. ***The Journal of Immunology,*** **2005, 175: 3252–3261.**

Measles virus (MV)[4] causes severe immune suppression followed by secondary infections that result in high rates of mortality of infants particularly in developing countries. Human CD46 (huCD46) (1, 2) and TLR-inducible human CD150 (huCD150) (3, 4) have been identified as MV receptors. Although huCD150 is the primary entry receptor for MV, it is not expressed in epithelial cells of the respiratory tract through which MV infection is known to initiate. The mechanism of wild-type MV spreading to systemic organs, therefore, remains unsolved.

No entry receptor for MV has been identified in mice. MV tropism is represented by its receptors, huCD46 and huCD150. Although rodents express the orthologues of these receptors, they fail to act as entry receptors for MV (2, 5, 6). MV infection of adult rodents is restricted to the brain-adapted strains obtained by intracerebral inoculations (7, 8). Transgenic (TG) mice expressing either huCD46 (9–11) or huCD150 (12, 13) have been established as models to investigate MV pathogenicity. Initially, most of the studies were performed using huCD46 TG mice. MV entry was found to be more efficient in mouse cells that express huCD46, the receptor for the MV vaccine Edmonston (ED) strain (1), and probably for several wild-type strains as well (14). However, TG rodents expressing huCD46 are not susceptible to MV infection when inoculated by routes other than intracerebral injection (15). Depletion of type I IFN receptors in the huCD46 TG mice led to high susceptibility to ED (16–18). These earlier studies, however, were performed before huCD150 was identified as the main receptor for wild-type MV strains (4). No in vivo studies have been attempted using wild-type MV strains and huCD46/huCD150 double TG mice for understanding the mechanisms of wild-type MV infection.

Using huCD150 single TG mice, several reports (12, 13) suggested that wild-type MV strains infect cells that constitutively express huCD150 but fail to induce systemic infection. huCD150 is inducible in human T cells and is up-regulated in myeloid dendritic cells (mDCs) and B cells in response to activation signaling from TLR (19–21). Thus, TG construct with just *lck* or CD11c

*Department of Immunology, Osaka Medical Center for Cancer and Cardiovascular Diseases, Osaka, Japan; †Department of Microbiology and Immunology, Graduate School of Medicine, Hokkaido University, Sapporo, Japan; ‡Genome Information Research Center, Osaka University, Suita, Osaka, Japan; §Department of Virology, Osaka City University Medical School, Osaka, Japan; and ¶Department of Immunology, Graduate School of Medicine and Faculty of Medicine, University of Tokyo, Tokyo, Japan

Received for publication February 4, 2005. Accepted for publication June 15, 2005.

The costs of publication of this article were defrayed in part by the payment of page charges. This article must therefore be hereby marked *advertisement* in accordance with 18 U.S.C. Section 1734 solely to indicate this fact.

[1] This work was supported in part by the Core Research for Evolutional Science and Technology (CREST), Japan Science and Technology Agency, by grants-in-aid from the Ministry of Education, Science, and Culture (Specified Project for Advanced Research), by the Ministry of Health and Welfare of Japan, the Naito Memorial Foundation (to M.M.), and by the Grant 11444 for graduate students from the Ministry of Education, Science, and Culture (to N.I.).

[2] M.S. and N.I. equally contributed to this work.

[3] Address correspondence and reprint requests to Dr. Tsukasa Seya, Department of Microbiology and Immunology, Graduate School of Medicine, Hokkaido University, Kita-ku, Sapporo 060-8637, Japan. E-mail address: seya-tu@med.hokudai.ac.jp

[4] Abbreviations used in this paper: MV, measles virus; BAC, bacterial artificial chromosome; CHO, Chinese hamster ovary; CYT, cytoplasmic tail; DC, dendritic cell; mDC, myeloid DC; pDC, plasmacytoid DC; ED, Edmonston; IC, Ichinose; IFNAR1, type I IFN-$\alpha\beta$ receptor; MALP, macrophage-activating lipopeptide; TG, transgenic; EGFP, enhanced GFP; MOI, multiplicity of infection; $TCID_{50}$, 50% tissue culture infective dose; IRF, IFN regulatory factor; CYT, cytoplasmic tail.

0022-1767/05/$02.00

promoter reported earlier (12, 13) may not be adequate for the study of natural huCD150 distribution, MV entry, and resultant infection via huCD150. Establishment of huCD46/huCD150 double TG mice with human-like distribution profile are necessary for the analysis of wild-type MV spreading and following host immunomodulatory events, particularly measles-mediated immune suppression (22–24).

Therefore, for this study, we generated huCD46/huCD150 double TG mice with or without type I IFN-$\alpha\beta$ receptor (IFNAR1). MV replication and spreading were surveyed by GFP-expressing wild-type Ichinose (IC) strain. In in vivo infection studies, however, neither type of MV was pathogenic to these TG mice irrespective of the route of administration. Analyses of these TG mice suggested that the critical factor in wild-type MV systemic infection appears to depend on the level of type I IFN generated by CD11c-positive dendritic cells (DCs) in this mouse model. In fact, DCs were infected with MV in the huCD150-positive TG mice with no IFNAR1. In this study, we first report that huCD46/huCD150 double TG mice are sensitive to wild-type MV once MV-infected mDCs are supplemented. Thus, infected mDCs facilitate establishing systemic MV infection in the TG mice. These double TG mice allow us to analyze immunomodulatory function of the MV receptors during MV infection (25, 26). The double TG mice with human-like huCD46/huCD150 expression profiles may be a better model for wild-type MV infection compared with huCD150 constitutively expressing mice.

Materials and Methods

Cell culture and reagents

Vero, Vero/huCD150 (a signaling lymphocyte activation molecule (SLAM)), which are Vero cells with stable expression of huCD150 obtained by transfection of huCD150/pCXN2 and antibiotic selection, HEK293, and 293-3-46 cells, kindly provided by M. A. Billeter (Institute of Molecular Biology, University of Zurich, Zurich, Switzerland) were maintained in DMEM supplemented with 10% heat-inactivated FCS and antibiotics. B95a cells were maintained in RPMI 1640 supplemented with 5% heat-inactivated FCS (JRH Biosciences) and antibiotics. Polymyxin B, LPS from *Escherichia coli* serotype O111:B4 was from Sigma-Aldrich. The mycoplasma lipopeptide macrophage-activating lipopeptide (MALP)-2 was prepared as described (27). MALP-2 was treated with polymyxin B (10 μg/ml) for 1 h at 37°C before stimulation of cells (27). Usually, 100 ng/ml LPS and 100 nM MALP-2 were used in mDC TLR stimulation. Isotype controls for PE rat IgG2a, PE rat IgG2b, PE mouse IgG1, PE or FITC golden syrian hamster IgG, FITC mouse IgG1, and FITC mouse IgG2a, and mAbs for PE anti-mouse CD8a, PE anti-mouse CD4, PE anti-mouse CD3e, PE anti-mouse CD19, PE anti-human CD3e, PE anti-human CD4, PE anti-human CD8a, PE anti-human CD19, and FITC anti-huCD150 were obtained from eBioscience. FITC or PE anti-mouse CD11c mAb was obtained from BD Pharmingen. FITC anti-huCD46 (MCP) mAb was obtained from Ancell. HRP-conjugated goat anti-rabbit Igs were obtained from American Qualex. Rabbit polyclonal bodies against huCD150 or huCD46 were produced in our laboratory.

TG method

Spermatozoa were dispersed from epididymis of 12-wk-old mature $B6D2F_1$ male mice in 400 μl of TYH medium diluted to 1×10^7/ml and frozen in liquid nitrogen immediately. The bacterial artificial chromosome (BAC) DNA carrying huCD46 or huCD150 was purchased from Incyte Genomics, and purified by using Large-Construct kit (Qiagen) according to the manufacturer's instructions. Each BAC DNA (5 μg/ml in TE buffer) was added to the thawed sperm. The mixtures were incubated for 5 min at room temperature, and mixed with one-tenth volume of 12% PVP-HCZB (polyvinyl-pyrrolidone-HEPES-Chatot, Ziamok, and Barister medium). The metaphase II oocytes for microinjection from $B6D2F_1$ female mice were prepared as previously described (28). These oocytes were maintained in kSOM (potassium simplex optimized medium) under mineral oil equilibrated in 5% (v/v) CO_2 in air at 37°C until use.

Generation of huCD46 and huCD150 TG mice

The huCD46 and huCD150 TG mice were produced by using the intracytoplasmic sperm injection transgene method (29). TG mice were made in accordance of the guidelines of the Animal Care and Use Committee of Osaka University. For microinjection, sperm heads were aspirated into a pipette attached to a piezoelectric pipette-driving unit and a sperm head was injected into each oocyte as previously described (28). After injection, the eggs were incubated in kSOM to the 2-cell stage, and were transferred to ICR pseudopregnant females. Among pups born, the huCD46 and huCD150 TG mice were detected by genomic PCR using huCD46- and huCD150-specific primers. The PCR primers used were as follows: 5′-AAAGGGCAAATTACCTTAGGGGTG-3′ and 5′-AGCACTTCGACC TAAAAATAGAGAT-3′ for huCD46 and 5′-GTGATACAGGAAGCG GGTTCAGG-3′, and 5′-GATACGCTGATTCCTGGCAGCTAAC-3′ for huCD150.

Southern blotting was performed with PCR products from human genome using those primers and with DIG High Prime DNA Labeling and Detection starter kit II (Roche Applied Science).

The $IFNAR1^{-/-}$ mouse (30) was obtained from The Jackson Laboratory. All mice were backcrossed at least six times to be a C57/BL6J background.

Western blotting

Various tissues from huCD46 and huCD150 TG mice were homogenized by a Potter-type homogenizer in 1% (v/v) Triton X-100, PBS, 1 mM PMSF, 10 mM benzamidine, 1 μg/ml pepstatin, and 1 μg/ml lepeptin. The extracts were centrifuged at 15,000 $\times$ *g*, and protein was estimated by Bio-Rad color reagent. A total of 20 μg of protein was subjected to SDS-PAGE under nonreducing conditions and transblotted onto nylon membranes. The membranes were incubated with anti-huCD46 polyclonal Ab or anti-huCD150 polyclonal Ab for 2 h, washed with PBS containing 0.5% Tween 20 three times and incubated with HRP-conjugated goat anti-rabbit Igs for 1 h at 37°C. Following second incubation, the membranes were washed three times with PBS-Tween 20 and proteins were detected with an ECL chemiluminescence kit (Amersham Biosciences).

Plasmid construction and rescue of recombinant viruses

For the preparation of wild-type MV IC-B strain (31, 32) expressing enhanced GFP (EGFP), we constructed p(+)MV323/GFP. Fragment 1, which has *Bss*HII site T7 promoter leader sequence with *Eco*RI site, was amplified by PCR with p(+)MV323/GFP as template using forward primer 5′-AGTCCGCGGGAgcgcgcGTAATACGACTCACTA-3′ (gcgcgc is *Bss*HII site and underline is T7 promoter), and reverse primer 5′-CG gaattcTCCCTAATCCTGCTCTTGTCCC-3′ (gaattc is *Eco*RI site and underline is a part of 5′ noncoding region of the N gene). Fragment 2, which has *Not*I site, the N gene terminator gene junction front half of the N gene with *Hin*dIII site, was amplified by PCR using p(+)MV323/GFP as template with forward primer 5′-CTgcggccgcATTGTTATAAAAAACTTAGG ATTCAAGATCCTATTA-3′ (gcggccgc is *Not*I site and underline is the N gene terminator, gene junction, and the N gene initiator) and reverse primer CCCaagcttCCTCTCGCACCTAGTCTAGAAGAT-3′ (aagctt is *Hin*dIII site and underline is a part of N gene coding region). The fragment 1 was digested with *Bss*HII and *Eco*RI, fragment 2 was digested with *Not*I and *Hin*dIII, and the EGFP gene was cut from pEGFP-N1 plasmid (Clontech Laboratories) with *Eco*RI and *Not*I. These three DNA fragments were ligated and the chimeric plasmid clone containing 5′ *Bss*HII site, T7 promoter, leader initiation signal (the 5′ region of the N gene) EGFP gene, and junction (a termination sequence of the 3′ region of the N gene/CTT sequence (the 5′ region of the N gene containing an initiation sequence), which have *Esp*I site) 3′ sequences, was generated. The accuracy of the fragment was confirmed by sequencing. The insert and p(+)MV323 were digested with *Bss*HII and *Esp*I, and the fragment containing an EGFP gene was inserted into p(+)MV323.

Recovery of infectious MV was performed as previously described (33, 34). MV323, MV323/GFP, and MV2A (ED strain) were recovered from p(+)MV323, p(+)MV323/GFP, and p(+)MV2A, respectively.

Immunofluorescence staining and confocal microscopy

Mock- or MV323GFP-infected mouse splenocytes were stained with PE rat IgG2a isotype control, PE rat IgG2b isotype control, PE golden syrian hamster IgG isotype control, PE anti-mouse CD8a mAb, PE anti-mouse CD4 mAb, PE anti-mouse CD3e mAb or PE anti-mouse CD19 mAb for 30 min at 4°C in FACS buffer. After washing, the stained cells were fixed in 0.5% formaldehyde in PBS and visualized at a magnification $\times$60 under a FLUOVIEW (Olympus). Images were captured using the attached computer FLUOVIEW software.

FACS cytometric analysis of cell surface Ags

FACS methods were previously described (35). Briefly, cells were suspended in PBS containing 0.1% sodium azide and 1% BSA (FACS buffer) and incubated for 30 min at 4°C with FITC-labeled mAbs and PE-labeled mAbs. Cells were washed and fluorescence intensity was measured by FACS.

Preparation of MV strains and in vitro MV infection analysis

Recovered viruses, MV2A (ED strain), MV323 (IC-B strain), and MV323GFP (IC-B strain containing EGFP gene), were passaged in B95a cells and titrated on Vero/SLAM cells. Low-passaged viruses were used in this experiment. The receptor usage of the strains was confirmed on Chinese hamster ovary (CHO), CHO/huCD46, or CHO/huCD150 cells (5). For in vitro viral infection assay, single cell suspensions of spleen from TG or non-TG littermates were obtained by passage thought sterile mesh. After removing erythrocytes using Lympholyte-M (Cedarlane Laboratories), purified cells were cultured in RPMI 1640 supplemented with 10% heat-inactivated FCS, 10 mM HEPES, 1 mM sodium pyruvate, 0.1 mM nonessential amino acids, 0.05 mM 2-ME, 50 U/ml mouse IL-2, 20 ng/ml PMA, and 1 μg/ml ionomycin for 24 h. FACS analysis was performed 48 h after infection.

Preparation of DCs

Mouse bone marrow-derived mDCs were prepared by the modified technique (36, 37) of earlier reported method (38). Briefly, 0.5–1 $\times$ 10^6 bone marrow cells/2 ml/well in RPMI 1640 supplemented with 10% heat-inactivated FCS, 10 mM HEPES, 1 mM sodium pyruvate, 0.1 mM nonessential amino acids, and 0.05 mM 2-ME were cultured overnight in 24-well plates. Nonadherent cells were harvested, resuspended in the same medium supplemented with 10 μg/ml mouse GM-CSF, and cultured in the mouse GM-CSF-containing medium. On day 3, adherent cells were cultured in fresh medium with 10 μg/ml mouse GM-CSF. On day 6, nonadherent cells and loosely adherent cells were harvested and used for experiments as immature DCs (38). Immature DCs were resuspended and cultured in fresh RPMI 1640 medium with 10 μg/ml mouse GM-CSF. Cellular RNA was estimated 24 h postinfection.

Human PBMC were isolated from buffy coat of normal healthy donors by methylcellulose sedimentation followed by standard density gradient centrifugation with Ficoll-Hypaque (Amersham Biosciences) (27). For human immature DC preparation, $CD14^+$ monocytes were obtained from human PBMC by using MACS system (Miltenyi Biotec) with anti-human CD14 mAb-conjugated microbeads and kept in RPMI 1640 (Invitrogen Life Technologies) containing 10% FCS, 500 IU/ml human GM-CSF, 100 IU/ml human IL-4 (PeproTech), and antibiotics for 6 days. Morphological changes were examined by phase contrast microscopy (Olympus IX-70).

Assay of in vivo MV infection

Newborn 2-day-old, 1-wk-old, or 6- to 10-wk-old TG or non-TG mice were injected i.p., i.v., intranasally, and s.c. with MV323GFP at a dose of 5×10^4 50% tissue culture infective doses ($TCID_{50}$). Mice were sacrificed 2–4 days after inoculation, and each tissue was collected and fixed with 4% paraformaldehyde in PBS overnight at 4°C. Tissues were embedded in Tissue-Tek OCT compound (Miles) and quickly frozen in liquid nitrogen. Serial frozen sections (10-μm thick) were cut with the cryostat (Leica) and were analyzed by confocal microscopy.

In vitro splenocytes proliferation assay

Splenocytes (1×10^5/100 μl/well in 96-well plate) freshly isolated from each TG mouse were stimulated with 20 ng/ml PMA and 1 μg/ml ionomycin in the presence of 50 U/ml mouse IL-2, and infected by MV323. Twenty-four hours later the cells were labeled for 16 h with [^{3}H]thymidine (1 mCi/ml). The incorporated counts were determined using a beta-plate reader in triplicate.

RT-PCR and quantitative PCR

Mouse mDCs or splenocytes were treated with trypsin and collected by centrifugation at 1500 $\times$ *g* for 10 min. Total RNA was extracted with RNeasy mini kit (Qiagen). A total of 2 μg of total RNA was incubated at 70°C for 5 min, kept on ice for 2 min, and reverse transcription was performed with Moloney murine leukemia virus-reverse transcriptase (Promega) at 37°C for 90 min followed by PCR or quantitative PCR. Following primers were used for PCR: α-IFN forward, 5′-AGTGATGAGCTAC TGGTCAAC-3′; reverse, 5′-TGATGCTGTGGAAGTATATCCTC-3′; β-IFN forward, 5′-TCCAGCTCCAAGAAAGGACG-3′; reverse, 5′-GCATCTTCTCCGTCATCTCC-3′; γ-IFN forward, 5′-AGACAGAAGT TCTGGGCTTCTC-3′; reverse, 5′-GGGTTGTTGACCTCAAACTTGG-3′; MV-H forward, 5′-CCCTTATCAACGGATGATCC-3′; reverse, 5′-GT GATCAATGGCCCGAATCC-3′; MV-N forward, 5′-AAGGTCAGTTC CACATT-3′; reverse, 5′-GAAGATCTCTGTCATTG-3′; IL-12 p40 forward, 5′-GAGTCATAGGCTCTGGAAAGACC-3′; reverse, 5′-AGTT GGGCAGGTGACATCC-3′; IL-10 forward, 5′-GGTTGCCAAGCCT TATCGGA-3′; reverse, 5′-ACCTGCTCCACTGCCTTGCT-3′; β-actin forward, 5′-ATCATGTTTGAGACCTTCAACACC-3′; reverse, 5′-GAT GTCACGCACGATTTCCC-3′; and HPRT (hypoxanthine phosphoribosyltransferase) forward, 5′-GTTGGATACAGGCCAGACTTTGTTG-3′, reverse, 5′-GAAGGGTAGGCTGGCCTATAGGCT-3′.

Reaction for quantitative PCR was done with iQ SYBER Green Supermix, and amplified PCR products were measured by iCycler iQ Real-Time PCR analyzing system (Bio-Rad). Normalized value for each mRNA expression was calculated as relative quantity of mRNA divided by the relative quantity of mouse hypoxanthine phosphoribosyltransferase.

Determination of human IFN-β level

Culture media were centrifuged to remove cell debris and supernatants were stored at −80°C until the assay. The level of secreted human IFN-β in the culture medium was determined with an ELISA kit (FUJIREBIO) for human IFN-β according to the manufacturer's protocol.

Results

Human-like expression of huCD46 or huCD150 in TG mice

Ubiquitous expression of huCD46 was not obtained in TG mice that were previously generated with huCD46 cDNA (39). A number of splicing variants in huCD46, which appeared in an organ-specific manner (40), participated in differential cell-mediated immune response (26). To generate the natural expression profile of huCD46 and its isoforms, we transferred the 194-kb BAC DNA carrying the huCD46 gene into mouse embryo and obtained TG mice with human-like CD46 expression pattern. Similarly, huCD150 TG mice were generated by transferring the huCD150 BAC DNA (185 kb) into mouse embryo. These mice have a human-like CD150 expression profile, which is inducible in T cells and up-regulated in mDCs and B cells. We examined the expression profiles of huCD46 and huCD150 in various organs of each line of our TG mice by SDS-PAGE and Western blotting (Fig. 1*A*). In huCD46 TG mice, huCD46 was ubiquitously expressed with the size variation of isoforms in an organ-specific fashion similar to human (41, 42). The brain of these mice notably expressed a low molecular mass moiety of huCD46 in the TG mice similar to human form. In addition, similar to human, huCD150 appeared in a tissue-specific manner in the thymus and spleen in huCD150 TG mice. In non-TG mice, no signals of huCD46 or huCD150 were detected in Western blots, suggesting no cross-reaction of the Abs with the mouse counterparts.

Cell populations expressing huCD46 or huCD150 in TG mice

We next analyzed cells from spleens of huCD46 TG, huCD150 TG, or non-TG mice by FACS analysis (Fig. 1*B*). In huCD46 TG mice, huCD46 was expressed on the surface of both CD3- or CD19-positive splenocytes. In huCD150 TG mice, huCD150 was expressed on CD19-positive cell surface, but minimal expression occurred on CD3-positive cells. Neither CD4 nor CD8 T cells expressed huCD150 (data not shown). Under similar FACS conditions, human PBMC ubiquitously expressed CD46 and partly expressed CD150 (Fig. 1*B*, *right*). When splenocytes from huCD150 TG mice were stimulated with PHA (data not shown) or PMA, ionomycin, and murine IL-2 (Fig. 1*C*, *left*), FACS profiles of the lymphocyte populations were altered. In addition, the levels of huCD150 in $CD4^+$ and $CD8^+$ T cell and $CD19^+$ B cell populations were up-regulated (Fig. 1*C*). Similar results were obtained with human PBMC when the cells were similarly stimulated (Fig. 1*C*, *right*). Neither huCD46 nor huCD150 was expressed in cells from non-TG mice as expected (see Fig. 5, *B* and *C*, labeled as

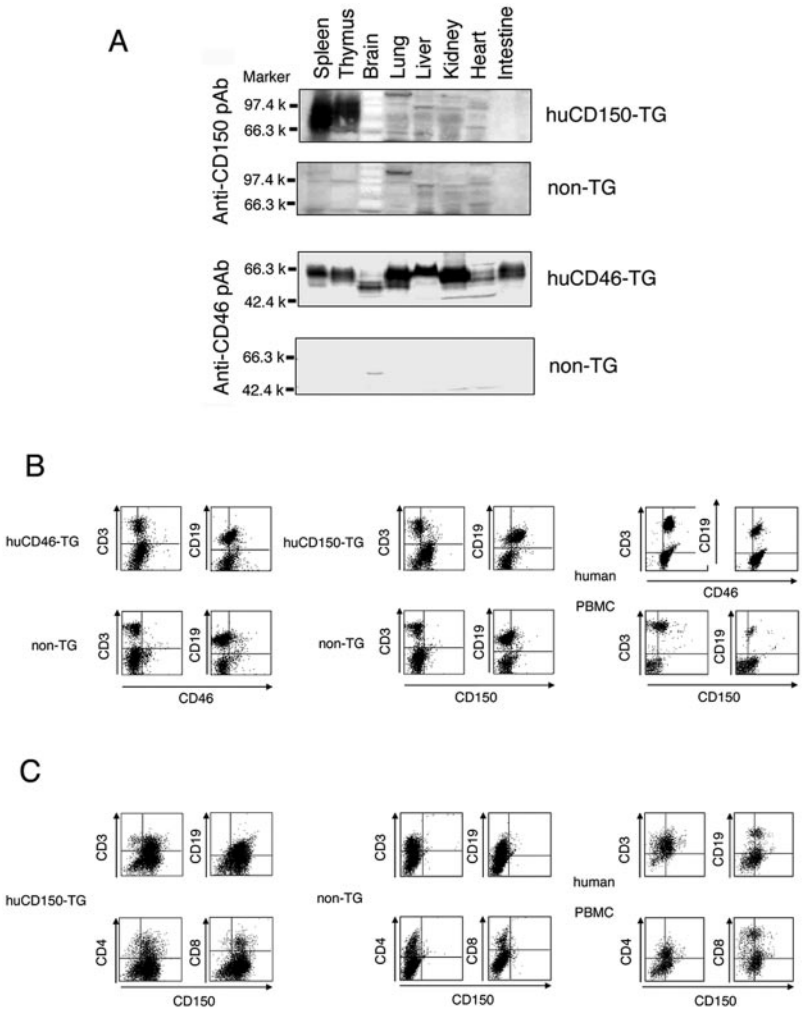

FIGURE 1. Generation of huCD46 and huCD150 TG mice. A, Western blot analysis of huCD46 and huCD150 in TG mice. Various tissues from huCD46 TG and huCD150 TG mice were homogenized and the extracts were separated by SDS-PAGE under nonreducing conditions and transblotted onto a nylon membrane. The huCD46 and huCD150 were then visualized with anti-human CD46 polyclonal Ab and anti-human CD150 polyclonal Ab, respectively, produced in our laboratory (64). *B* and *C*, FACS analysis for detection of huCD46 and huCD150 in mouse spleen cell populations and human PBMC. Freshly isolated splenocytes from the huCD46 and huCD150 TG mice or human PBMC were stained with FITC-labeled anti-human CD46 or CD150 mAb, and PE-labeled mCD3, mCD4, mCD8, or mCD19 mAb before (*B*) or after (*C*) stimulation with PMA and ionomycin.

"non-TG"). These results show that huCD150-inducible TG mice were established, which may suit the study for susceptibility of cell species to MV strains.

We then generated huCD46/huCD150 double TG mice by mating both TG lines (Fig. 2*A*). Gene analysis showed that the littermates of huCD46/huCD150 TG, huCD46 TG, huCD150 TG, and non-TG mice followed Mendel's laws of inheritance (Fig. 2*A*), suggesting that huCD46/huCD150 transgene does not bring about any lethal defect. The presence of huCD46 and huCD150 genes in litters was monitored by PCR (data not shown) and confirmed by Southern blot analysis (Fig. 2*B*). Expression profiles of huCD46 and huCD150 in each litter were also confirmed by Western blot and FACS analysis (data not shown).

Preparation of EGFP-labeled MV

To monitor MV infection, we generated EGFP-expressing recombinant MV (IC323GFP) based on the wild-type IC strain. Plasmid containing full-length cDNA of the IC strain and the EGFP gene was constructed as shown in Fig. 3*A*. GFP expression reflects viral replication in this construct. The rescued MV323GFP showed almost the same growth kinetics as the parental recombinant MV323. Its receptor usage was confirmed with CHO cells expressing huCD46 or huCD150 (Fig. 3*B*). MV2A (ED strain) rescued from p(+)MV2A, was used as the laboratory-adapted strain. When infected with MV2A, both CHO/huCD46 and CHO/huCD150 cells produced the typical syncytia, whereas MV323 infected CHO/huCD150 cells but not CHO/huCD46 cells (data not shown). MV323GFP also infected CHO/huCD150 cells to form syncytia exhibiting green autofluorescence, but did not form any syncytium in CHO/huCD46 and intact CHO cells.

In vitro analysis of MV infection of splenocytes from TG mice

To examine in vitro MV infection, the splenocytes were isolated from each TG mouse and infected with MV323GFP at a multiplicity of infection (MOI) of 0.25 (Fig. 4*A*). When prestimulated with PMA and ionomycin, some splenocytes from the double TG or huCD150 TG mice were positive in GFP, a marker for infection. The stimulation was essential for MV permissiveness as reported before (14). However, under any infectious conditions the splenocytes from huCD46 TG and non-TG mice were GFP-negative. The results were confirmed to be reproducible by semiquantitative FACS analysis (Fig. 4*A*). In contrast, MV323GFP infected human PBMC even at low MOI of inoculation (Fig. 4*A*, *bottom panels*). Human PBMC appear to be more susceptible to MV323GFP than the splenocytes of the double TG and huCD150 TG mice.

To examine which populations of splenocytes of huCD46/huCD150 TG or huCD150 TG mice were infected with MV323GFP, we segregated them with PE-conjugated anti-mouse CD3, CD4, CD8, CD11c, or CD19 mAb and analyzed them by FACS and confocal microscopy (Fig. 4, *B* and *C*). MV323GFP inoculation rendered the CD3-, CD4-, CD8-, and CD19-positive cells green. But CD11c-positive cells barely turned green even at

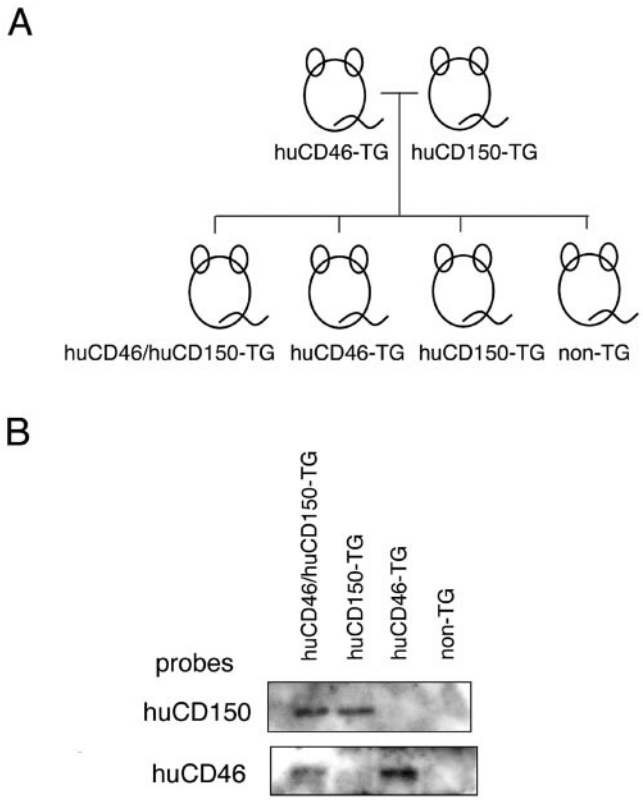

FIGURE 2. Scheme for generation of double TG mice and confirmation of genotypes. *A*, Heterogenic human CD46 and human CD150 TG mice were mated, and Mandelian inheritance of the offspring of huCD46/huCD150, huCD46, huCD150 is diagrammatically represented. *B*, Southern blots of gene transfer profiles of double TG mice.

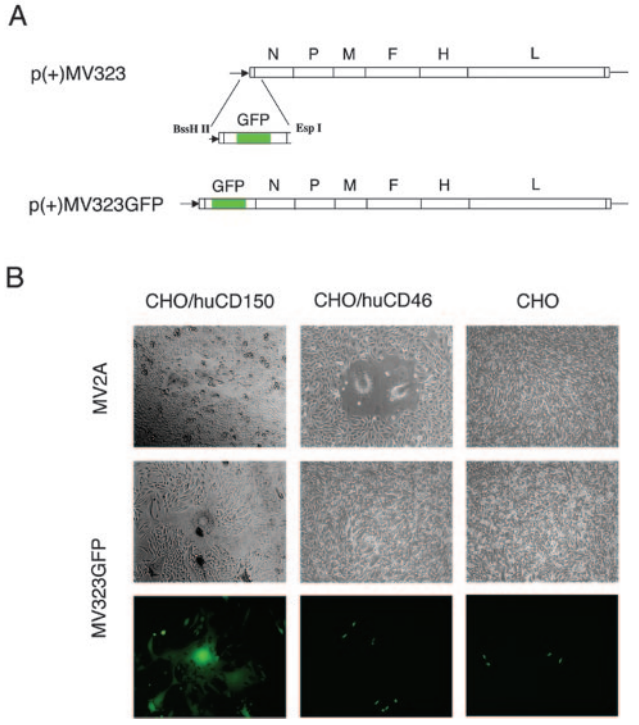

FIGURE 3. Generation of EGFP-labeled wild-type MV (MV323GFP). *A*, Scheme for GFP-labeled MV323 (MV323GFP) construction shows the p(+)MV323 plasmid (*upper*) coding wild-type MV IC strain antigenome and a construct of EGFP. The EGFP construct was placed upstream of the N gene of IC. The construct of p(+)MV323GFP that expresses GFP and viral proteins is also shown (*lower*). *B*, Receptor usage of MV323GFP. Rescued virus MV323GFP from p(+)MV323GFP was inoculated on CHO/huCD150, CHO/huCD46, and intact CHO cells, and 2 days later receptor tropism of MV323GFP was confirmed by syncytium formation and GFP fluorescence. MV2A (ED strain) rescued from p(+)MV2A was used as a control that can use both receptors. Magnification, ×100.

high MOI inoculation (Fig. 4*B*). Thus, the CD11c-positive splenocytes that are representative of DCs are less susceptible to wild-type MV compared with other cell types.

Wild-type MV fails to infect the TG mice in vivo

Next we examined in vivo MV infection. Six- to 10-wk-old double TG, huCD150 TG, huCD46 TG, or non-TG mice were injected i.p., i.v., intranasally, or s.c. with MV323GFP at a dose of 5×10^4 to 1×10^6 $TCID_{50}$. None of the TG mice showed any sign of illness. Two to 4 days after inoculation, the sections of brain, spleen, thymus, lymph nodes, lung, kidney, liver, intestine, and heart from each mouse were examined for GFP-positive cells to monitor infection by MV323GFP. No GFP-positive cells were detected in any tissue. Following i.p. injection of MV323GFP in newborn 2-day-old or 1-wk-old TG or normal mice, no GFP was detected. Intravenously transferred MV323GFP-infected splenocytes to double TG mouse also did not show any GFP-positive lesions (data not shown).

MV fails to effectively replicate in mouse DC

It was reported earlier that huCD150 were minimally expressed in human monocyte-derived DCs and up-regulated by stimulation of TLRs (20). We confirmed the expression and up-regulation of huCD150 in mDCs from huCD46/huCD150 TG mice (Fig. 5*A*). mDCs prepared from the TG mice by conventional method (the purity confirmed by the CD11c marker) expressed both huCD150 and huCD46 with a pattern similar to human monocyte-derived DCs. When mDCs were stimulated with LPS, a ligand of TLR4, expression of huCD150 was up-regulated. Similar huCD150 up-regulation was observed by stimulation with MALP-2, which is a ligand of TLR2. Of note, the level of huCD46 was not influenced in mDC in which TLRs were stimulated.

Because GFP-positive cells reflecting MV323GFP infection were barely detected in CD11c-positive splenocytes (Fig. 4*B*), we examined whether mDCs prepared from TG or non-TG mice were susceptible to MV. The mDCs from each TG mouse line were inoculated with MV323GFP at MOI = 0.25 (Fig. 5*B*). Only a few GFP-positive cells were found in mDCs from the double TG (Fig. 5*B*, left) and huCD150 TG, but not huCD46 TG and non-TG mice (data not shown). The results were compared with human monocyte-derived DCs. At MOI = 0.25 (Fig. 5*B*, *right*), a number of human DCs turned GFP-positive.

We have reported that human DCs were more susceptible to wild-type MV strains than were the laboratory-adapted and vaccine strains (20). The difference was caused by the ability of MV strains to induce type I IFN in DCs (43, 44). Human monocyte-derived DCs were inoculated with MV323, MV2A, or mock viruses at MOI = 1, whereas human IFN-β was actually produced in culture supernatants as measured by ELISA. As expected, human DCs infected with MV323 produced lower levels of IFN-β than did DCs infected with MV2A (Fig. 6*A*). Then, we examined type I IFN levels in culture supernatants of mDCs challenged with wild-type strain MV323. mDCs prepared from each TG mouse line were incubated with the same lots of MV strains at MOI = 1, and mouse IFN-β mRNA levels were measured by quantitative PCR (Fig. 6*B*). When MV323 infected mDCs from huCD46/huCD150

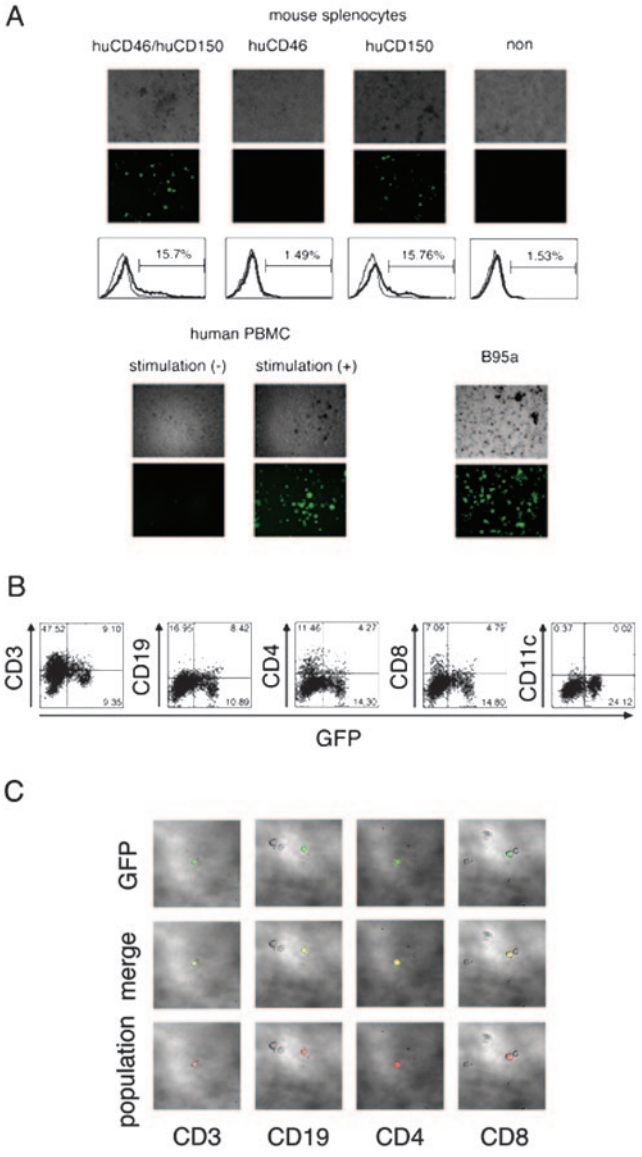

FIGURE 4. In vitro and ex vivo analysis for MV323GFP infection in splenocytes from TG mice. The splenocytes isolated from each TG mouse were stimulated with or without PMA, ionomycin, and, IL-2 and infected with MV323GFP at MOI = 0.25 for 2 days. Cells were observed by fluorescence microscope (*A*), FACS (*B*), and confocal microscope (*C*). *A*, Human PBMC and B95a cells were used as controls. B95a cells were not prestimulated, whereas either stimulated or unstimulated human PBMC and mouse splenocytes were used for infection studies. Magnification, ×40. Infectivity of splenocytes from the indicated mouse line was measured by FACS analysis (*bottom*). Fluorescence intensity reflects the levels of the MV-associated GFP. *B*, Positive cell populations (*inset*) are shown as a percentage. *C*, GFP (infected cells, green) are indicated (*upper*) and the splenocyte populations (CDs, red) are indicated (*lower*). Their merging profiles (yellow) are also shown (*middle*). Magnification, ×200.

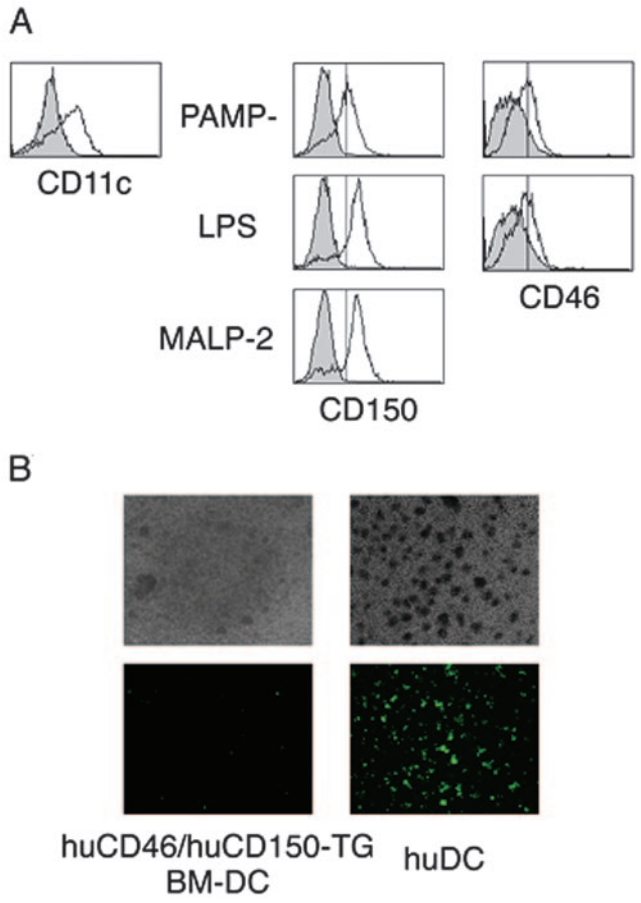

FIGURE 5. Expression profiles of huCD46 and huCD150 and testing MV sensitivity of mDCs. *A*, huCD46 and huCD150 on CD11c-positive mDCs. The expression of CD11c, huCD46, and huCD150 in mDCs prepared from huCD46/huCD150 TG mice were examined using FACS. TLR4 agonist (LPS) and TLR2 agonist (MALP-2) were used as mDC maturation inducers. Control mDCs (PAMP−) were cultured without any TLR stimulator. *B*, Efficacy of MV infection in human monocyte-derived DCs and mDC prepared from the double TG mice. mDCs from each mouse line and human monocyte-derived DCs were infected with MV323GFP at MOI = 0.25. Two days later, cells were observed under fluorescence microscope. Magnification, ×40.

TG and huCD150 TG, the mRNA levels of type-I IFN (IFN-α and IFN-β) were markedly increased in the mDCs (Fig. 6, *B* and *C*). MV2A induced IFN-α and IFN-β in the mDCs from double TG, huCD150 TG, and huCD46 TG (Fig. 6, *B* and *C*). Induction of IFN-α was less compared with IFN-β. In mouse blood cells, however, neither IFN-β nor IFN-α message was virtually detected: only a trace amount of IFN-γ message was measurable (data not shown). Local, rather than systemic, induction of type I IFN-β would occur by mDCs in response to wild-type MV. The levels of total IFN-β production depend on the combined actions of MV strain types and IFN inducibility of mDCs. Because IL-12 p40 and IL-10 were induced from human DCs as a consequence of MV infection, we also measured the mRNA level of murine IL-12 p40 and murine IL-10 of mDCs (Fig. 6, *D* and *E*). Results showed that the mRNAs of these cytokines were also induced by MV infection via the MV receptors. MV infection was confirmed by determination of the mRNA level of the H protein gene of MV (Fig. 6*F*). Although the same lots of virus stocks were used for infection, MV323 replicated better in mDCs from huCD150 TG than huCD46/huCD150 TG mouse lines. MV2A replication was high in mDCs from huCD150 TG and low in mDCs from the double TG and huCD46 TG mouse lines. The coexpressed huCD46 would probably inhibit viral replication in mouse mDCs.

DC have critical role in the establishment of MV infection in vivo

Differential susceptibility to MV of mDCs prepared from huCD46/huCD150 TG mouse vs human DCs earlier described, allowed us to speculate that DCs play a critical role in the development of systemic MV infection in vivo. Because type I IFN induced by

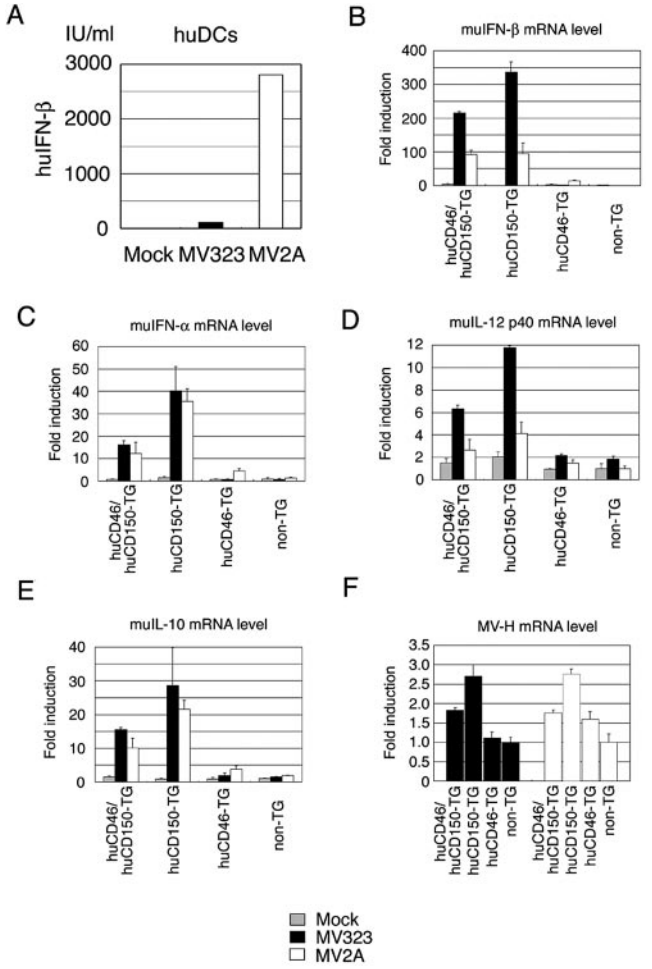

FIGURE 6. MV-induced molecules and cytokines in mouse bone-marrow-derived mDCs. Cytokine induction and MV replication profiles in mDCs prepared from TG mouse lines. *A*, Human monocyte-derived DCs were infected with MV323 or MV2A at MOI = 1. At 24 h after infection the levels of human IFN-β in the supernatants were measured using ELISA. *B*, mDCs were prepared from each indicated TG mouse line and infected with MV323 or MV2A at MOI = 1. At 24 h after infection, the mRNA levels of mouse IFN-β affected by infection with MV323 or MV2A in mDCs were measured by quantitative PCR. Fold induction against mock infection in non-TG is shown. *C–F*, mDCs prepared as in *A* and *B* were similarly infected with MV323 or MV2A at MOI = 1. At 24 h after infection, the mRNA levels of mouse (mu) IFN-α (*C*), IL-12 p40 (*D*), IL-10 (*E*), and MV-H (*F*) were measured by quantitative PCR. Relative fold induction against mock infection in non-TG is shown. The experiments were performed at least three times and represented results are shown.

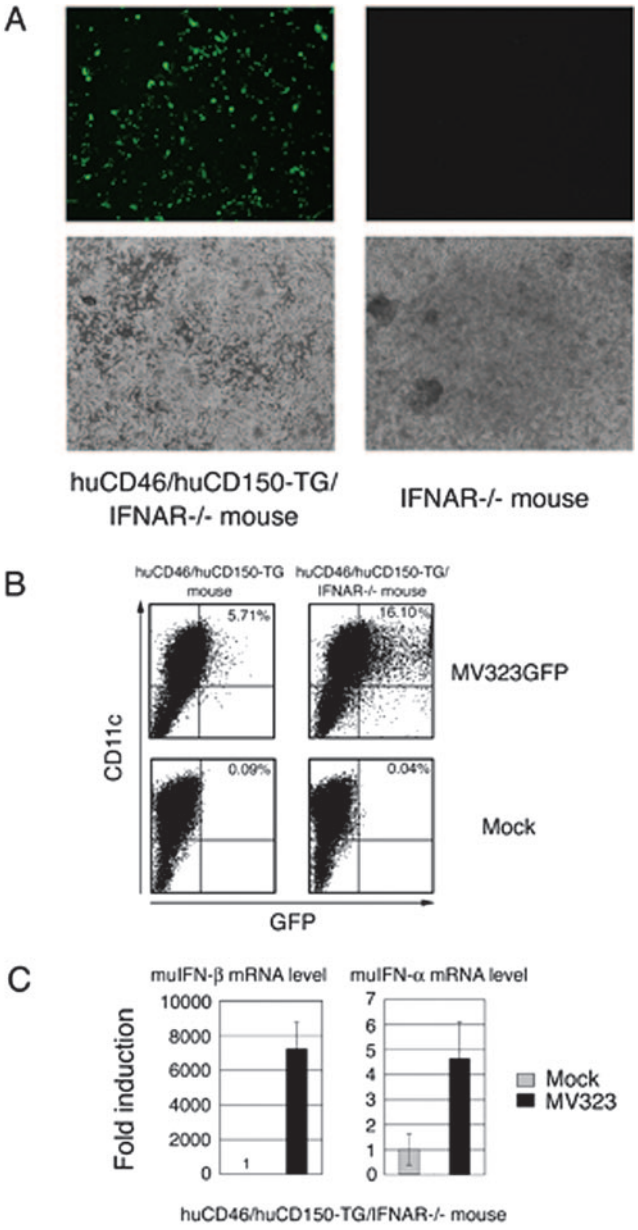

FIGURE 7. mDCs from huCD46/huCD150 TG/IFNAR$^{-/-}$ mice are susceptible against MV infection. *A*, mDCs susceptible to MV. mDCs prepared from huCD46/huCD150 TG/IFNAR$^{-/-}$ mice or IFNAR$^{-/-}$ mice (control) were inoculated with MV323GFP at MOI = 0.25. At 24 h later, cells were observed under fluorescence microscope. Magnification, ×40. *B*, mDCs from huCD46/huCD150 TG and huCD46/huCD150 TG/IFNAR$^{-/-}$ mouse prepared as in *A* were infected with MV323GFP at MOI = 0.25. At 24 h later, cells were stained with PE-labeled mouse CD11c and measured by FACS analysis. *C*, mDCs prepared as in *A* were infected with mock or MV323GFP for 24 h at MOI = 1. The mRNA levels of mouse IFN-β and IFN-α were measured by quantitative PCR. Relative fold induction against mock infection is shown.

wild-type MV acted on huCD46/huCD150-positive mDCs in a positive feedback manner, we generated huCD150/huCD46/IFNAR1$^{-/-}$ triple mutant mice, by mating the double TG mice with the IFN $\alpha\beta$ receptor 1 (IFNAR1) knockout mouse. First, we examined whether mDCs from huCD150/huCD46/IFNAR1$^{-/-}$ mutant mice were susceptible to wild-type MV infection in vitro. When the mDCs were inoculated with MV323GFP at MOI = 0.25, many GFP-positive mDCs were detected by fluorescence microscopy (Fig. 7*A*) and FACS analysis (Fig. 7*B*). Moreover, robust type I IFN production was detected in mDCs (Fig. 7*C*). The mDCs were incubated with MV323 at MOI = 1 for 24 h, and then the mRNA levels of mouse IFN-β and IFN-α were measured using quantitative PCR. As viral replication increased, IFN-β production also increased (Fig. 7, *B* and *C*). IFN-α production was largely suppressed because of the lack of the secondary signal via IFNAR1 (Fig. 7*B*, *right*). Because mDCs in triple mutant mice became susceptible to wild-type MV, we next analyzed the results of in vivo MV infection. For this, the triple mutant mice were injected i.p. with MV323GFP at a dose of 5×10^4 $TCID_{50}$. Two days later, some of the tissues were collected and their sections were directly observed by inverted fluorescence microscope (Fig. 8*A*). GFP-positive cells were detected in mesenteric lymph nodes, inguinal lymph nodes, parathymic lymph nodes, and spleen. Yet,

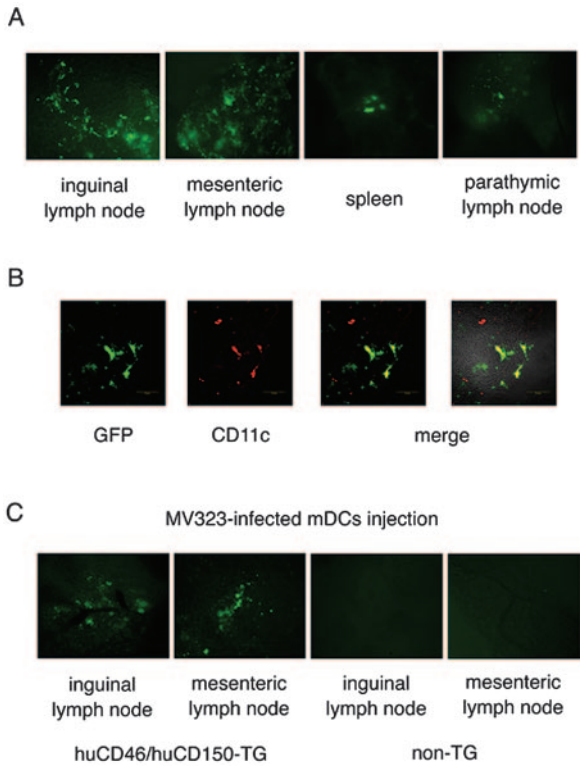

FIGURE 8. mDCs participate in systemic viral spreading. *A*, MV infection visualized in the triple mutant mice by in vivo inoculation of MV323GFP. Representative photographic images of GFP-positive organs in huCD46/huCD150 TG/IFNAR$^{-/-}$ mice are shown. At 48 h after i.p. injection of 10^5 $TCID_{50}$ of MV323GFP, the mice were dissected and tissues were directly examined under an inverted fluorescence microscope. Magnification, ×100. *B*, CD11c-positive cells reserve MV323GFP. Mesenteric lymph nodes were fixed with 4% paraformaldehyde and the sections were stained with PE-conjugated anti-mouse CD11c mAb (red). EGFP (green) and CD11c (red) were observed by confocal microscopy. Merging profiles are shown to the *right*. Magnification, ×400. *C*, MV infection visualized by transfer of MV-infected mDCs into IFNAR1$^{+/+}$ TG mice. mDCs prepared from huCD46/huCD150 TG/IFNAR$^{-/-}$ mice were infected with MV323GFP at MOI = 1. At 24 h later, MV323GFP-infected mDCs (1×10^6) were i.v. injected into huCD46/huCD150 TG, huCD46 TG, huCD150 TG, and non-TG mice (IFNAR1 is normal in all TG mice). Two days later, each mouse was dissected and tissues were directly examined under an inverted fluorescence microscope. Magnification, ×100. The results were confirmed by two additional experiments.

no positive cells were found in brain, thymus, lung, heart, liver, kidney or intestine.

We prepared sections from mesenteric lymph nodes, and stained with PE-conjugated anti-mouse CD11c mAb. As shown in Fig. 8*B*, GFP-positive and CD11c-positive cells merged in the lymph nodes. Thus, we speculated that MV-infected mDCs delivered viruses to local draining lymph nodes. To confirm this hypothesis, we i.v. transferred MV323GFP-infected mDCs (1×10^6 cells, MOI = 1) from huCD150/huCD46/IFNAR1$^{-/-}$ mice to huCD46/huCD150, huCD150, huCD46, or non-TG mice (IFNAR1 is normal in each mouse strain). Two days later, the affected mice were dissected and specified tissues were directly observed by inverted fluorescence microscope (Fig. 8*C*). In mesenteric and inguinal lymph nodes from huCD46/huCD150 TG and huCD150 TG mice, GFP-positive lesions were detected. No such lesions were observed in affected huCD46 TG and non-TG mice. Based on these results, we infer that in this model MV-infected mDCs facilitate establishing systemic MV infection. IFNAR1$^{-/-}$ mDCs allowing viral replication inside the cells, trigger successive viral delivering to lymph nodes.

Discussion

We generated TG mice that express MV receptors huCD46 and huCD150. The expression profiles and the distribution of these receptors in these mice were similar to those in humans. Mouse splenocytes from the double TG mice became susceptible to wild-type MV strains in vitro. Nevertheless, despite the fact that the TG mice expressed both huCD46/huCD150, they were highly resisted MV infection in vivo irrespective of the route of MV administration. huCD150 but not huCD46 was up-regulated in response to TLR stimulators and conferred high susceptibility to wild-type MV on mDCs. In vivo, normal CD11c-positive DCs were usually insensitive to wild-type MV infection, whereas these DCs turned susceptible to MV if their amplifiable IFN-inducing ability in response to MV infection was spoiled. Systemic MV infection was observed in the huCD46/huCD150 double TG mice with no IFNAR1 by direct MV injection or in the double TG mice with normal IFNAR1 by transfer of MV-infected mDC to them. Thus, in vivo MV permissiveness was accomplished when the IFNAR1 gene was simultaneously disrupted in DCs.

A crucial question remains elusive that this TG mice model with natural expression profile of huCD46 and huCD150 serve as a model for the investigation of human wild-type MV infection. Different from human, IFNAR1$^{-/-}$ mice induce basal production of IFN-β in response to IFN regulatory factor (IRF)-3 activation, but secondary amplifiable response is severely impaired (45, 46). Opposing to the results on human DC, mouse mDC more efficiently induce type I IFN in response to infection by wild-type MV than to infection by attenuated MV strains (Fig. 6). Wild-type MV strains barely induce amplified type I IFN production in human DCs, whereas attenuated strains robustly induce it (M. Taniguchi, N. Begum, and T. Seya, unpublished observation). Thus, pathogenicity of wild-type MV strains may not be reflected in our mouse model. MV strains, either wild-type or laboratory-adapted, appear to replicate well in human DCs if they induce only minute degrees of type I IFN (20). We would say that our mouse model in part reflects MV infection of humans whether we choose MV strains with lesser ability to induce IFN-β or choose to activate the secondary amplified type I IFN pathway. Further study is needed to confirm these issues.

Which of CD11c-positive DCs, mDCs, or pDCs play a major role in MV-mediated IFN induction is a critical question. Both mDC and pDC are CD11c-positive and possess the pathways that induce IFN type I in response to RNA viruses (47). Our infection study on mouse mDC is: 1) MV more prominently induces IFN-β than IFN-α in IC-infected double TG mice (Fig. 7, *C* and *D*); 2) double TG mice without IFNAR1 induced an extremely lower level of IFN-α as compared with the TG mice with normal IFNAR1 (Figs. 7*C* and 8*B*). This is true in human in which wild-type MV strains efficiently replicate in DCs and barely induce type I IFN (20, 43). Recent reports after the submission of our study clearly revealed that the MyD88-IRF-7 pathway in pDC is the main route of IFN-α induction in mice in several virus species (48, 49). Perhaps, mDC induces IFN-β via Toll-IL-1R homology domain-containing adapter molecule 1-mediated or RNA helicase RIG-I-mediated IRF-3 activation pathways, which is independent of MyD88-dependent IRF-7 activation pathway. We could test this issue regarding MV if the mouse IFN-α and IFN–β are separately determined by ELISA. At least blood cells barely induce the messages of type I IFN in response to MV infection (data not shown), and the role of pDC in our mouse MV infection model remain to

be settled. Further MV infection studies using mice disrupting either of the IFN-inducing pathways will be required to clarify the source of type I IFN in MV-infected TG mice.

Wild-type MV-H protein acts as a ligand for TLR2 (2) and up-regulates CD150 in human monocytes (50). Although in vitro analysis speculated that DC matures into a stage vulnerable to wild-type MV through TLR2 signaling (51), whether wild-type MV actually infects mDC in vivo remains undetermined. Our mouse model offers the possibility that the matured DC is the primary target of wild-type MV strains. Testing the role of TLR2 by MV-H protein stimulation in immature DC maturation is feasible in our model. Dysfunction of Ag-presenting capacity of DC through MV infection may be associated with modulation of TLR signaling by MV.

Previous reports suggested that MV efficiently infected human DC and suppressed DC-mediated allostimulatory lymphocyte proliferation (MLR) (52–54). Both wild-type and vaccine strains induce defective MLR response irrespective of the induction levels of type I IFNs. Testing MLR in intact vs MV-infected mDCs prepared from these TG mice will give us a hint to resolve DC-based immune suppression. The model may enable us to test the role of huCD150 and/or huCD46 on lymphocytes in association with infected mDCs.

A comparison of the double TG mice with huCD150 TG mice in their ability to produce differential cytokine levels suggests that huCD150 TG mice more efficiently induce all four cytokines tested than do huCD46/huCD150 TG mice (Fig. 6, *B–E*). The replication level of MV-H was high in huCD150 TG mice and relatively low in huCD46/huCD150 TG mice (Fig. 6*F*). The results suggest that CD46 expressed on mDCs acts as a negative regulator for wild-type MV replication. According to previous reports, mouse macrophages expressing human CD46 significantly resist MV infection (55). These cells produced high levels of NO and IFN-$\alpha\beta$ upon infection by MV (55, 56), suggesting that huCD46 enhances IFN-$\alpha\beta$ production in mouse macrophages. Thus, it is possible that simultaneous expression of huCD46 and huCD150 in mDC down-regulates MV replication. Alternatively, huCD46 in lymphocytes deliver negative or positive signal in lymphoproliferation depending on the type of tail sequences as reported previously (25, 26). There are two major isoforms of huCD46 with differential cytoplasmic tails (CYTs), CYT1 and CYT2 (25, 57). NO is induced in macrophages in a CYT1>CYT2 fashion (55, 58). In mouse lymphocytes from TG mice with either CYT1 or CYT2, differential functions of these isoforms were clearly observed (26). Relationship between the huCD46 isoforms and IFN-β production will be an issue to be tested in our model.

In human myeloid DCs, TLR3 and TLR8 participate in type I IFN production (59). Mouse mDCs lack TLR8 (60, 61). RIG-I participates in sensing viral infection inside the cells to activate a signaling pathway for induction of type I IFN (62). Yet, TLR3 may sense viral infection, as in West Nile virus entry into the brain (63). Human monocytes may express CD150 in the adenoid tissue to catch up inspired MV (50). Therefore, interpretation of differential responses between mouse mDC and human immature DC in wild *vs* vaccine strains need to take these recent findings into consideration. It is important to further analyze the natural intranasal infection of MV and its relationship to the properties of wild-type MV-infected CD11c-positive mDCs.

Our findings can be summarized as follows: 1) mouse CD11c-positive mDCs in huCD46/huCD150 double TG mice are barely susceptible to wild-type MV until IFNAR1 is depleted; 2) in the double TG mice with no IFNAR1, only CD11c-positive mDCs are vulnerable to MV at an early phase of infection in vivo; 3) robust IFN type I induction due to IFNAR1 by mDCs confers natural resistance to wild-type MV on mice; and 4) the huCD46/huCD150 double TG mouse when injected with MV-infected mDCs i.v. permits systemic infection by MV. Therefore, in this mouse model mDC carries MV to draining lymph nodes. Although the results were deduced from an artificial model case, the TG mice with or without IFNAR1 would be applicable for the study of MV-mediated initial IFN-β induction in mDC. With these mice, virus-mediated initial IFN-β inducing response and its related pathways involving IRF-3 and IRF-7 in mDCs may be critically analyzed. This is the first report on the generation of wild-type MV-sensitive mice.

Acknowledgments

We are grateful to Drs. K. Toyoshima, N. Inoue, M. Tanabe K. Funami, T. Tsujita (Osaka Medical Center for Cancer, Osaka, Japan), M. Ikawa (Osaka University), Y. Seto (Osaka City University), M. Kohanawa (Hokkaido University, Sapporo, Japan), and A. Takaoka (University of Tokyo, Tokyo, Japan) for helpful discussions. Thanks are also due to K. Shida, Y. Okuda, M. Sasai, A. Matsuo, and H. Masuda (Osaka Medical Center for Cancer) for helpful technical support. We thank Dr. M. A. Billeter (University of Zurich) for kindly providing p(+)MV2A plasmid and MV rescue system from cDNA and Dr. K. Takeuchi (Tsukuba University, Ibaragi, Japan) for kindly providing p(+)MV323 plasmid.

Disclosures

The authors have no financial conflict of interest.

References

1. Dorig, R. E., A. Marcil, A. Chopra, and C. D. Richardson. 1993. The human CD46 molecule is a receptor for measles virus (Edmonston strain). *Cell* 75: 295–305.
2. Naniche, D., G. Varior-Krishnan, F. Cervoni, T. F. Wild, B. Rossi, C. Rabourdin-Combe, and D. Gerlier. 1993. Human membrane cofactor protein (CD46) acts as a cellular receptor for measles virus. *J. Virol.* 67: 6025–6032.
3. Hsu, E. C., C. Iorio, F. Sarangi, A. A. Khine, and C. D. Richardson. 2001. CDw150(SLAM) is a receptor for a lymphotropic strain of measles virus and may account for the immunosuppressive properties of this virus. *Virology* 279: 9–21.
4. Tatsuo, H., N. Ono, K. Tanaka, and Y. Yanagi. 2000. SLAM (CDw150) is a cellular receptor for measles virus. *Nature* 406: 893–897.
5. Ono, N., H. Tatsuo, K. Tanaka, H. Minagawa, and Y. Yanagi. 2001. V domain of human SLAM (CDw150) is essential for its function as a measles virus receptor. *J. Virol.* 75: 1594–1600.
6. Tsujimura, A., K. Shida, M. Kitamura, M. Nomura, J. Takeda, H. Tanaka, M. Matsumoto, K. Matsumiya, A. Okuyama, Y. Nishimune, et al. 1998. Molecular cloning of a murine homologue of membrane cofactor protein (CD46): preferential expression in testicular germ cells. *Biochem. J.* 330(Pt. 1): 163–168.
7. Liebert, U. G., and D. Finke. 1995. Measles virus infections in rodents. *Curr. Top. Microbiol. Immunol.* 191: 149–166.
8. Rima, B. K., J. A. Earle, K. Baczko, P. A. Rota, and W. J. Bellini. 1995. Measles virus strain variations. *Curr. Top. Microbiol. Immunol.* 191: 65–83.
9. Horvat, B., P. Rivailler, G. Varior-Krishnan, A. Cardoso, D. Gerlier, and C. Rabourdin-Combe. 1996. Transgenic mice expressing human measles virus (MV) receptor CD46 provide cells exhibiting different permissivities to MV infections. *J. Virol.* 70: 6673–6681.
10. Oldstone, M. B., H. Lewicki, D. Thomas, A. Tishon, S. Dales, J. Patterson, M. Manchester, D. Homann, D. Naniche, and A. Holz. 1999. Measles virus infection in a transgenic model: virus-induced immunosuppression and central nervous system disease. *Cell* 98: 629–640.
11. Rall, G. F., M. Manchester, L. R. Daniels, E. M. Callahan, A. R. Belman, and M. B. Oldstone. 1997. A transgenic mouse model for measles virus infection of the brain. *Proc. Natl. Acad. Sci. USA* 94: 4659–4663.
12. Hahm, B., N. Arbour, D. Naniche, D. Homann, M. Manchester, and M. B. Oldstone. 2003. Measles virus infects and suppresses proliferation of T lymphocytes from transgenic mice bearing human signaling lymphocytic activation molecule. *J. Virol.* 77: 3505–3515.
13. Hahm, B., N. Arbour, and M. B. Oldstone. 2004. Measles virus interacts with human SLAM receptor on dendritic cells to cause immunosuppression. *Virology* 323: 292–302.
14. Manchester, M., D. S. Eto, A. Valsamakis, P. B. Liton, R. Fernandez-Munoz, P. A. Rota, W. J. Bellini, D. N. Forthal, and M. B. Oldstone. 2000. Clinical isolates of measles virus use CD46 as a cellular receptor. *J. Virol.* 74: 3967–3974.
15. Manchester, M., and G. F. Rall. 2001. Model systems: transgenic mouse models for measles pathogenesis. *Trends Microbiol.* 9: 19–23.
16. Mrkic, B., J. Pavlovic, T. Rulicke, P. Volpe, C. J. Buchholz, D. Hourcade, J. P. Atkinson, A. Aguzzi, and R. Cattaneo. 1998. Measles virus spread and pathogenesis in genetically modified mice. *J. Virol.* 72: 7420–7427.
17. Mrkic, B., B. Odermatt, M. A. Klein, M. A. Billeter, J. Pavlovic, and R. Cattaneo. 2000. Lymphatic dissemination and comparative pathology of recombinant measles viruses in genetically modified mice. *J. Virol.* 74: 1364–1372.

18. Peng, K. W., M. Frenzke, R. Myers, D. Soeffker, M. Harvey, S. Greiner, E. Galanis, R. Cattaneo, M. J. Federspiel, and S. J. Russell. 2003. Biodistribution of oncolytic measles virus after intraperitoneal administration into Ifnar-CD46Ge transgenic mice. *Hum. Gene Ther.* 14: 1565–1577.
19. Cocks, B. G., C. C. Chang, J. M. Carballido, H. Yssel, J. E. de Vries, and G. Aversa. 1995. A novel receptor involved in T-cell activation. *Nature* 376: 260–263.
20. Murabayashi, N., M. Kurita-Taniguchi, M. Ayata, M. Matsumoto, H. Ogura, and T. Seya. 2002. Susceptibility of human dendritic cells (DCs) to measles virus (MV) depends on their activation stages in conjunction with the level of CDw150: role of Toll stimulators in DC maturation and MV amplification. *Microbes Infect.* 4: 785–794.
21. Sidorenko, S. P., and E. A. Clark. 1993. Characterization of a cell surface glycoprotein IPO-3, expressed on activated human B and T lymphocytes. *J. Immunol.* 151: 4614–4624.
22. Karp, C. L. 1999. Measles: immunosuppression, interleukin-12, and complement receptors. *Immunol. Rev.* 168: 91–101.
23. Klagge, I. M., V. ter Meulen, and S. Schneider-Schaulies. 2000. Measles virus-induced promotion of dendritic cell maturation by soluble mediators does not overcome the immunosuppressive activity of viral glycoproteins on the cell surface. *Eur. J. Immunol.* 30: 2741–2750.
24. Schneider-Schaulies, S., S. Niewiesk, J. Schneider-Schaulies, and V. ter Meulen. 2001. Measles virus induced immunosuppression: targets and effector mechanisms. *Curr. Mol. Med.* 1: 163–181.
25. Kemper, C., A. C. Chan, J. M. Green, K. A. Brett, K. M. Murphy, and J. P. Atkinson. 2003. Activation of human $CD4^+$ cells with CD3 and CD46 induces a T-regulatory cell 1 phenotype. *Nature* 421: 388–392.
26. Marie, J. C., A. L. Astier, P. Rivailler, C. Rabourdin-Combe, T. F. Wild, and B. Horvat. 2002. Linking innate and acquired immunity: divergent role of CD46 cytoplasmic domains in T cell induced inflammation. *Nat. Immunol.* 3: 659–666.
27. Nishiguchi, M., M. Matsumoto, T. Takao, M. Hoshino, Y. Shimonishi, S. Tsuji, N. A. Begum, O. Takeuchi, S. Akira, K. Toyoshima, and T. Seya. 2001. *Mycoplasma fermentans* lipoprotein M161Ag-induced cell activation is mediated by Toll-like receptor 2: role of N-terminal hydrophobic portion in its multiple functions. *J. Immunol.* 166: 2610–2616.
28. Kimura, Y., and R. Yanagimachi. 1995. Intracytoplasmic sperm injection in the mouse. *Biol. Reprod.* 52: 709–720.
29. Perry, A. C., T. Wakayama, H. Kishikawa, T. Kasai, M. Okabe, Y. Toyoda, and R. Yanagimachi. 1999. Mammalian transgenesis by intracytoplasmic sperm injection. *Science* 284: 1180–1183.
30. Muller, U., U. Steinhoff, L. F. Reis, S. Hemmi, J. Pavlovic, R. M. Zinkernagel, and M. Aguet. 1994. Functional role of type I and type II interferons in antiviral defense. *Science* 264: 1918–1921.
31. Takeuchi, K., N. Miyajima, F. Kobune, and M. Tashiro. 2000. Comparative nucleotide sequence analyses of the entire genomes of B95a cell-isolated and Vero cell-isolated measles viruses from the same patient. *Virus Genes* 20: 253–257.
32. Kobune, F., H. Sakata, and A. Sugiura. 1990. Marmoset lymphoblastoid cells as a sensitive host for isolation of measles virus. *J. Virol.* 64: 700–705.
33. Radecke, F., P. Spielhofer, H. Schneider, K. Kaelin, M. Huber, C. Dotsch, G. Christiansen, and M. A. Billeter. 1995. Rescue of measles viruses from cloned DNA. *EMBO J.* 14: 5773–5784.
34. Takeda, M., K. Takeuchi, N. Miyajima, F. Kobune, Y. Ami, N. Nagata, Y. Suzaki, Y. Nagai, and M. Tashiro. 2000. Recovery of pathogenic measles virus from cloned cDNA. *J. Virol.* 74: 6643–6647.
35. Tsuji, S., M. Matsumoto, O. Takeuchi, S. Akira, I. Azuma, A. Hayashi, K. Toyoshima, and T. Seya. 2000. Maturation of human dendritic cells by cell wall skeleton of *Mycobacterium bovis* bacillus Calmette-Guerin: involvement of Toll-like receptors. *Infect. Immun.* 68: 6883–6890.
36. Akazawa, T., H. Masuda, Y. Saeki, M. Matsumoto, K. Takeda, K. Tsujimura, K. Kuzushima, T. Takahashi, I. Azuma, S. Akira, K. Toyoshima, and T. Seya. 2004. Adjuvant-mediated tumor regression and tumor-specific cytotoxic response are impaired in MyD88-deficient mice. *Cancer Res.* 64: 757–764.
37. Kaisho, T., O. Takeuchi, T. Kawai, K. Hoshino, and S. Akira. 2001. Endotoxin-induced maturation of MyD88-deficient dendritic cells. *J. Immunol.* 166: 5688–5694.
38. Inaba, K., M. Pack, M. Inaba, H. Sakuta, F. Isdell, and R. M. Steinman. 1997. High levels of a major histocompatibility complex II-self peptide complex on dendritic cells from the T cell areas of lymph nodes. *J. Exp. Med.* 186: 665–672.
39. Miyagawa, S., S. Mikata, H. Tanaka, M. Ikawa, K. Kominami, T. Seya, Y. Nishimune, R. Shirakura, and M. Okabe. 1997. The regulation of membrane cofactor protein (CD46) expression by the 3′ untranslated region in transgenic mice. *Biochem. Biophys. Res. Commun.* 233: 829–833.
40. Johnstone, R. W., B. E. Loveland, and I. F. McKenzie. 1993. Identification and quantification of complement regulator CD46 on normal human tissues. *Immunology* 79: 341–347.
41. Inoue, N., A. Fukui, H. Oshiumi, M. Matsumoto, and T. Seya. 1999. Method for production of human CD46 transgenic mice. *Host Defense* 8: 27 (*Abstr.*).
42. Kemper, C., M. Leung, C. B. Stephensen, C. A. Pinkert, M. K. Liszewski, R. Cattaneo, and J. P. Atkinson. 2001. Membrane cofactor protein (MCP; CD46) expression in transgenic mice. *Clin. Exp. Immunol.* 124: 180–189.
43. Naniche, D., A. Yeh, D. Eto, M. Manchester, R. M. Friedman, and M. B. Oldstone. 2000. Evasion of host defenses by measles virus: wild-type measles virus infection interferes with induction of α/β interferon production. *J. Virol.* 74: 7478–7484.
44. Tanabe, M., M. Kurita-Taniguchi, K. Takeuchi, M. Takeda, M. Shingai, M. Ayata, H. Ogura, M. Matsumoto, and T. Seya. 2003. Mechanism of up-regulation of human Toll-like receptor (TLR) 3 secondary to infection of measles virus attenuated strains. *Biochem. Biophys. Res. Commun.* 311: 39–48.
45. Taniguchi, T., and A. Takaoka. 2002. The interferon-α/β system in antiviral responses: a multimodal machinery of gene regulation by the IRF family of transcription factors. *Curr. Opin. Immunol.* 14: 111–116.
46. Jiang, Z., T. W. Mak, G. Sen, and X. Li. 2004. Toll-like receptor 3-mediated activation of NF-κB and IRF3 diverges at Toll-IL-1 receptor domain-containing adapter inducing IFN-β. *Proc. Natl. Acad. Sci. USA* 101: 3533–3538.
47. Sato, A., and A. Iwasaki. 2004. Induction of antiviral immunity requires Toll-like receptor signaling in both stromal and dendritic cell compartments. *Proc. Natl. Acad. Sci. USA* 101: 16274–16279.
48. Kawai, T., S. Sato, K. J. Ishii, C. Coban, H. Hemmi, M. Yamamoto, K. Terai, M. Matsuda, J. Inoue, S. Uematsu, et al. 2004. Interferon-α induction through Toll-like receptors involves a direct interaction of IRF7 with MyD88 and TRAF6. *Nat. Immunol.* 10: 1061–1068.
49. Honda, K., H. Yanai, H. Negishi, M. Asagiri, M. Sato, T. Mizutani, N. Shimada, Y. Ohba, A. Takaoka, N. Yoshida, and T. Taniguchi. 2005. IRF-7 is the master regulator of type-I interferon-dependent immune responses. *Nature* 434: 772–777.
50. Minagawa, H., K. Tanaka, N. Ono, H. Tatsuo, and Y. Yanagi. 2001. Induction of the measles virus receptor SLAM (CD150) on monocytes. *J. Gen. Virol.* 82(Pt. 12): 2913–2917.
51. Bieback, K., E. Lien, I. M. Klagge, E. Avota, J. Schneider-Schaulies, W. P. Duprex, H. Wagner, C. J. Kirschning, V. Ter Meulen, and S. Schneider-Schaulies. 2002. Hemagglutinin protein of wild-type measles virus activates Toll-like receptor 2 signaling. *J. Virol.* 76: 8729–8736.
52. Fugier-Vivier, I., C. Servet-Delprat, P. Rivailler, M. C. Rissoan, Y. J. Liu, and C. Rabourdin-Combe. 1997. Measles virus suppresses cell-mediated immunity by interfering with the survival and functions of dendritic and T cells. *J. Exp. Med.* 186: 813–823.
53. Grosjean, I., C. Caux, C. Bella, I. Berger, F. Wild, J. Banchereau, and D. Kaiserlian. 1997. Measles virus infects human dendritic cells and blocks their allostimulatory properties for $CD4^+$ T cells. *J. Exp. Med.* 186: 801–812.
54. Schlender, J., J. J. Schnorr, P. Spielhoffer, T. Cathomen, R. Cattaneo, M. A. Billeter, V. ter Meulen, and S. Schneider-Schaulies. 1996. Interaction of measles virus glycoproteins with the surface of uninfected peripheral blood lymphocytes induces immunosuppression in vitro. *Proc. Natl. Acad. Sci. USA* 93: 13194–13194.
55. Hirano, A., Z. Yang, Y. Katayama, J. Korte-Sarfaty, and T. C. Wong. 1999. Human CD46 enhances nitric oxide production in mouse macrophages in response to measles virus infection in the presence of γ interferon: dependence on the CD46 cytoplasmic domains. *J. Virol.* 73: 4776–4785.
56. Katayama, Y., A. Hirano, and T. C. Wong. 2000. Human receptor for measles virus (CD46) enhances nitric oxide production and restricts virus replication in mouse macrophages by modulating production of α/β interferon. *J. Virol.* 74: 1252–1257.
57. Seya, T., and S. Nagasawa. 2001. CD46: membrane cofactor protein of complement and a measles virus receptor. In *Encyclopedia of Molecular Medicine*. T. E. Creighton, ed. John Wiley & Sons, Inc. New York, NY, p. 628.
58. Hirano, A., M. Kurita-Taniguchi, Y. Katayama, M. Matsumoto, T. C. Wong, and T. Seya. 2002. Ligation of human CD46 with purified complement C3b or $F(ab')_2$ of monoclonal antibodies enhances isoform-specific interferon γ-dependent nitric oxide production in macrophages. *J. Biochem.* 132: 83–91.
59. Jurk, M., F. Heil, J. Vollmer, C. Schetter, A. M. Krieg, H. Wagner, G. Lipford, and S. Bauer. 2002. Human TLR7 or TLR8 independently confer responsiveness to the antiviral compound R-848. *Nat. Immunol.* 3: 499.
60. Heil, F., H. Hemmi, H. Hochrein, F. Ampenberger, C. Kirschning, S. Akira, G. Lipford, H. Wagner, and S. Bauer. 2004. Species-specific recognition of single-stranded RNA via Toll-like receptor 7 and 8. *Science* 303: 1526–1529.
61. Coccia, E. M., M. Severa, E. Giacomini, D. Monneron, M. E. Remoli, I. Julkunen, M. Cella, R. Lande, and G. Uze. 2004. Viral infection and Toll-like receptor agonists induce a differential expression of type I and λ interferons in human plasmacytoid and monocyte-derived dendritic cells. *Eur. J. Immunol.* 34: 796–805.
62. Yoneyama, M., M. Kikuchi, T. Natsukawa, N. Shinobu, T. Imaizumi, M. Miyagishi, K. Taira, S. Akira, and T. Fujita. 2004. The RNA helicase RIG-I has an essential function in double-stranded RNA-induced innate antiviral responses. *Nat. Immunol.* 5: 730–737.
63. Wang, T., T. Town, L. Alexopoulou, J. F. Anderson, E. Fikrig, and R. A. Flavell. 2004. Toll-like receptor 3 mediates West Nile virus entry into the brain causing lethal encephalitis. *Nat. Med.* 10: 1366–1373.
64. Kurita-Taniguchi, M., A. Fukui, K. Hazeki, A. Hirano, S. Tsuji, M. Watanabe, M. Matsumoto, S. Ueda, and T. Seya. 2000. Functional modulation of human macrophages through CD46 (measles virus receptor): production of IL-12 p40 and nitric oxide in association with recruitment of SHP-1 to CD46. *J. Immunol.* 165: 5143–5152.